Suplemento de la Revista Mexicana de Física **3** 040916 (2022) 1–6

Heavy Flavor Physics at the EIC with the ECCE detector

Xuan Li on behalf of the ECCE consortium
Physics division, Los Alamos National Laboratory, Los Alamos, NM, 87545, USA.

Received 3 July 2022; accepted 15 September 2022

The proposed Electron-Ion Collider (EIC) will operate high-energy high-luminosity electron+proton and electron+nucleus collisions to solve several unresolved fundamental questions. Due to their large masses ($m_{c,b} > \Lambda_{QCD}$), heavy quarks and their hadron products are ideal probes to study the nucleon/nuclear parton distribution functions in the high Bjorken-x ($x_{BJ} > 0.1$) region and explore the hadronization process within the unconstrained kinematic region. Recently, the Electron-Ion Collider Comprehensive Chromodynamics Experiment (ECCE) consortium detector conceptual design has been selected as the reference design for the EIC project detector. The precise momentum and spatial resolutions provided by the ECCE tracking detector enable a series of open heavy flavor and quarkonia measurements. The physics projections of these proposed heavy flavor measurements in simulation studies using the ECCE detector design will be presented.

Keywords: ***Electron-Ion Collider, Heavy Flavor, Quarkonia, Parton Fragmentation, Hadronization***

1 Introduction

The next generation Quantum Chromodynamics (QCD) accelerator: Electron-Ion Collider (EIC) has received the Critical Decision 1 (CD1) approval in 2021 with the determination of its alternative selection and cost range from the US Department of Energy (DOE). The EIC will operate $e + p$ and $e + A$ collisions at the center of mass energies from 40 to 141 GeV and the instantaneous luminosity can reach $10^{33-34} cm^{-2} s^{-1}$. These unique features bring new opportunities to precisely study the nucleon/nuclei 3D structure, help address the proton spin puzzle, probe the nucleon/nuclei parton density extreme: the gluon saturation, and explore how quarks and gluon form visible matter, which is referred to as the hadronization [1, 2]. In $e + p$ and $e + A$ collisions, heavy quarks are produced through the photon-gluon fusion in the leading order Deeply Inelastic Scattering (DIS) process. On the other hand, heavy quarks will not transfer into other quarks and gluons once they are produced due to their heavy masses. Therefore, the heavy flavor hadrons and jets are ideal probes to access the gluon parton distribution functions within the less constrained high Bjorken-x region ($x_{BJ} > 0.1$) and systematically explore the heavy quark fragmentation process in the high hadron momentum fraction region ($z_h > 0.4$).

Heavy flavor hadrons such as D^0 mesons usually have relatively short lifetime ($c\tau_0 < 600\ \mu m$) and decay into other lighter particles. In experiments, the displaced/decay vertex or the track Distance of Closet Approach (DCA), which is proportional to the particle decay length, is one of the key parameters to identify heavy flavor hadrons. To realize precise heavy flavor measurements, the detector is required to meet these requirements: 1) providing fine spatial resolution ($< 100\ \mu m$) for displaced vertex reconstruction or DCA 2) having low material budgets to maintain fine track hit resolution and offer good track momentum resolutions, and 3) providing good particle identification to suppress the combinatorial background.

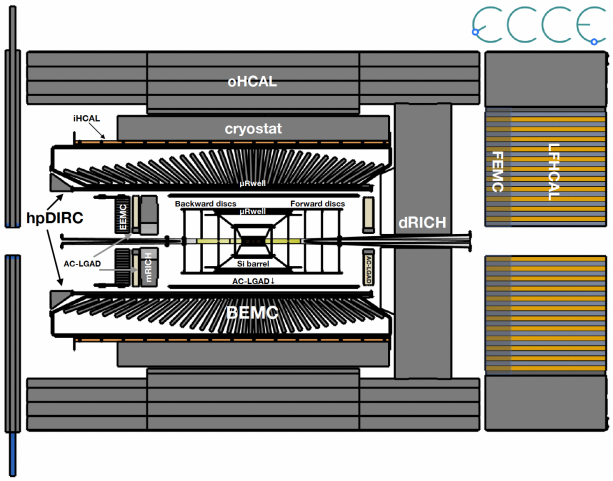

FIGURE 1. The schematic of the ECCE conceptual detector design, which reuses the 1.4 T Babar magnet. The ECCE central detector is divided into the barrel, hadron-endcap and electron-endcap kinematic regions. It consists of the Monolithic Active Pixel Sensor (MAPS) based silicon vertex/tracking detector, the micron-Rwell (μRwell) Based gas tracking detector, the AC-LGAD based Time of Fight, dRICH, mRICH, ElectroMagnetic (EM) Calorimeter, and Hadronic Calorimeter.

The Electron-Ion Collider Comprehensive Chromodynamics Experiment (ECCE) consortium has developed a conceptual design, which consists of vertex, tracking, particle identification (PID) and calorimeter subsystems to meet various EIC physics requirements listed in the EIC white paper [1] and the EIC yellow report [2]. As shown in Figure 1, the ECCE conceptual detector design consists of multiple layers of different detector subsystems, which can provide precise particle vertex, tracking, identification, momentum and energy measure-

ments in the pseudorapidity region of $-3.5 \leq \eta \leq 3.5$ with full azimuthal coverage. The ECCE vertex and tracking detectors play an essential role in the heavy flavor hadron and jet reconstruction. The geometry parameters of the ECCE vertex and tracking detector reference design are listed in Table I.

In addition to the fine segmentation of the ECCE tracking detector active area, a service cone which includes the estimated material budgets associate with cables, cooling and support structures has been implemented into the full GEANT4 [3] simulation within the Fun4All framework [4,5] for the tracking performance evaluation. A critical kinematic variable for the heavy flavor reconstruction is the track transverse Distance of Closest Approach (DCA_{2D}), which is proportional to the heavy flavor particle decay length. Good tracking momentum resolutions and fine transverse DCA resolutions can be achieved the ECCE vertex and tracking detector, which utilizes advanced silicon and gas tracking technologies. The DCA_{2D} resolutions of the ECCE detector design can meet or even perform better than the EIC yellow report requirements [2] as shown as the dashed lines in Figure 2. To optimize the ECCE detector configuration, several iterations have been carried out to implement different detector geometries and alternative technology options. The associated tracking performance of different detector configurations has been included in the systematic uncertainty evaluation.

TABLE I. ECCE vertex and tracking detector geometry

Region/ Technology	Index	r (cm)	z_{min} (cm)	z_{max} (cm)
barrel				
MAPS	1	3.3	-13.5	13.5
MAPS	2	4.35	-13.5	13.5
MAPS	3	5.4	-13.5	13.5
MAPS	4	21	-27	27
MAPS	5	22.68	-30	30
μ RWELL	6	33.14	-40	40
μ RWELL	7	51	-106	106
AC-LGAD	8	64	-140	140
μ RWELL	9	77	-197	145
		z (cm)	r_{in} (cm)	r_{out} (cm)
h-endcap				
MAPS	1	25	3.5	18.5
MAPS	2	49	3.5	36.5
MAPS	3	73	4.5	40.5
MAPS	4	106	5.5	41.5
MAPS	5	125	7.5	43.5
AC-LGAD	6	182	7	87
e-endcap				
MAPS	1	-25	3.5	18.5
MAPS	2	-52	3.5	36.5
MAPS	3	-79	4.5	40.5
MAPS	4	-106	5.5	41.5
AC-LGAD	5	-155.5	8	64

Several heavy flavor hadron and jet reconstructions have been studied in $e+p$ simulation through the newly developed analysis framework, which consists of the PYTHIA 8 event generation [6]; smeared particle vertex, tracking and energy information based on the performance of the ECCE conceptual detector design, which is determined from the GEANT4 simulation; the EIC electron and proton/nucleus beam crossing angle at 25 $mrad$; and the beam remnant backgrounds. We will present the heavy flavor reconstruction in simulation and associated physics projections in the following sections.

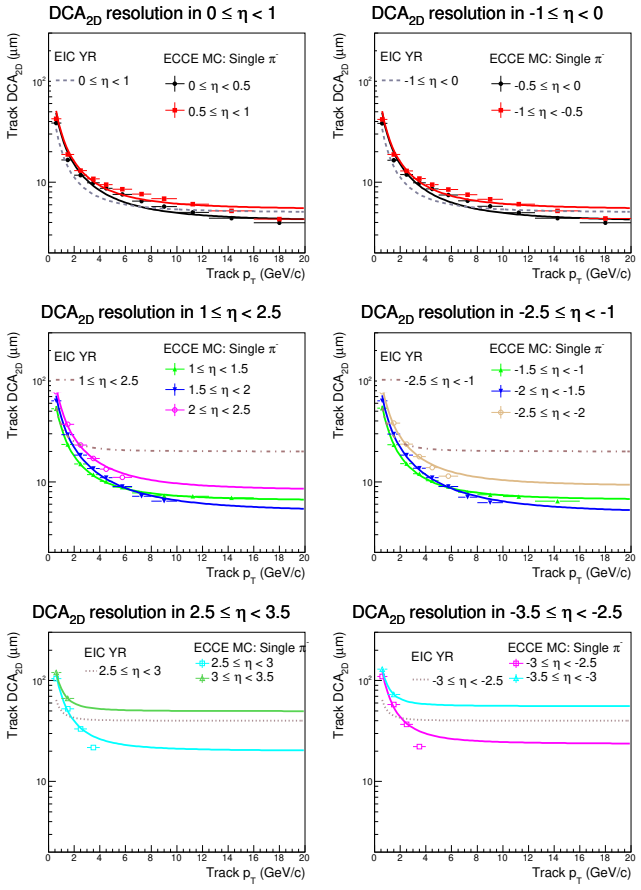

FIGURE 2. Track transverse momentum dependent transverse Distance of Closet Approach (DCA_{2D}) resolutions in the $0 \leq \eta \leq 3.5$ (left column) and $-3.5 \leq \eta < 0$ (right column) pseudorapidity regions with the ECCE conceptual detector design and the 1.4 T Babar magnet. The EIC yellow report requirements are highlighted in dashed lines.

2 Heavy flavor hadron and jet reconstruction

The open heavy flavor hadron reconstruction has been carried out in $e+p$ simulation with the electron beam energy at 10 GeV and the proton beam energy at 100 GeV. Several topological cuts, which include the DCA_{2D} matching between heavy flavor decay particle candidates and constraints on the crossing angle between the reconstructed heavy flavor

DCA vector and its momenta, have been applied to enhance the signal over background ratios.

Figure 3 shows the mass distributions of reconstructed $D^{\pm}$, $D^0(\bar{D}^0)$, $B^{\pm}$, $B^0(\bar{B}^0)$ and $B_s^0(\bar{B}_s^0)$ mesons in simulation using the ECCE reference detector design with the 10 fb^{-1} integrated luminosity of 10 GeV electron and 100 GeV proton collisions. With the optimized topological cuts, good signal over background ratios have been obtained for reconstructed D-mesons and B-mesons as illustrated in Figure 3. 10 fb^{-1} is a estimated minimal value of the integrated luminosity to be delivered by one year EIC operation. The good statistics of reconstructed D-mesons allow us to further study their kinematic dependence nuclear modification factor measurements.

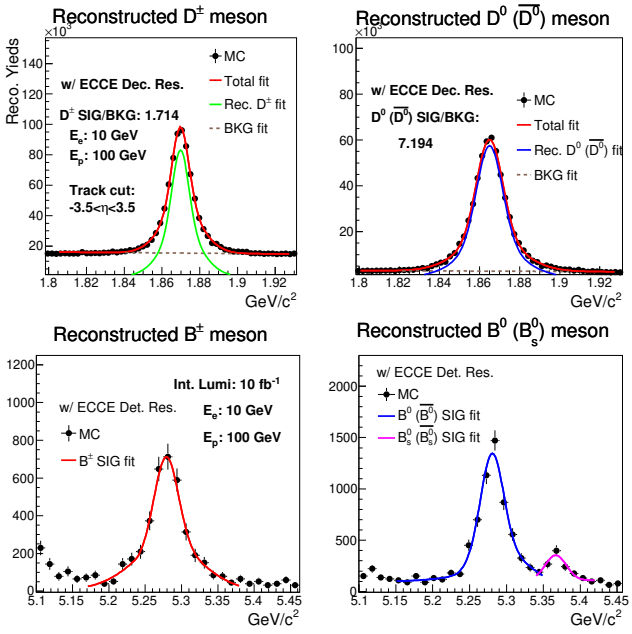

FIGURE 3. Reconstructed heavy flavor hadron mass distributions with the ECCE reference detector design performance inside the 1.4 T Babar magnet within the presudorapidity region of $-3.5 \leq \eta \leq 3.5$ in 10+100 GeV $e+p$ collisions. The integrated luminosity is 10 fb^{-1}. The distributions of reconstructed $D^{\pm}$ and $D^0(\bar{D}^0)$ mesons are shown in the top row and the distributions of reconstructed $B^{\pm}$, $B^0(\bar{B}^0)$ and $B_s^0(\bar{B}_s^0)$ mesons are shown in the bottom row.

Figure 4 illustrates the pseudorapdity separated reconstructed $D^0(\bar{D}^0)$ mass spectrums in the $e+p$ simulation with the ECCE reference detector design with 10 fb^{-1} integrated luminosity of $e+p$ collisions at 63.2 GeV. These distributions are divided into three pseudorapidity bins, $-2 < \eta \leq 0$ (backward region), $0 < \eta \leq 2$ (central region), and $2 < \eta \leq 3.5$ (forward region). The signal over background ratio of reconstructed $D^0(\bar{D}^0)$ mesons reduces as the reconstructed $D^0(\bar{D}^0)$ presudorapdity increases. This is due to the combined effects from reduced charm hadron cross section from the central to the forward and backward pseudrapidity regions, better tracking momentum resolutions in the central pseudrapidity region than the forward and backward pseudrapidity regions and the kinematics of $D^0(\bar{D}^0)$ decay particles.

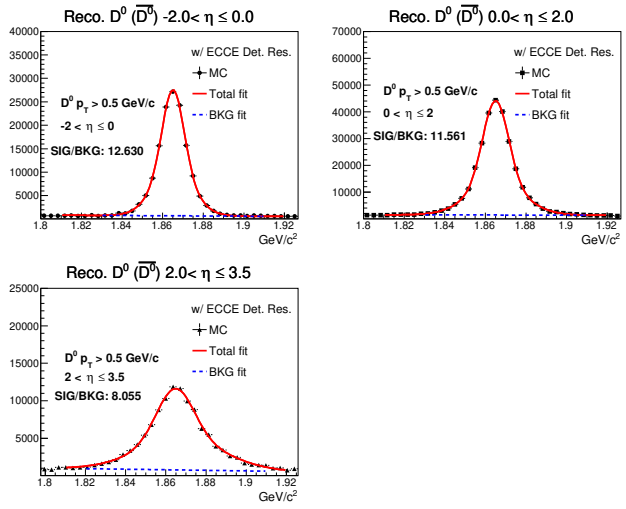

FIGURE 4. Reconstructed D^0 ($\bar{D}^0$) mass distributions in $-2 < \eta \leq 0$ (top left), $0 < \eta \leq 2$ (top right), and $2 < \eta \leq 3.5$ (bottom left) pseudorapidity regions in 10+100 GeV $e+p$ simulation with the ECCE reference detector design performance and the 1.4 T Babar magnet. The integrated luminosity is 10 fb^{-1}.

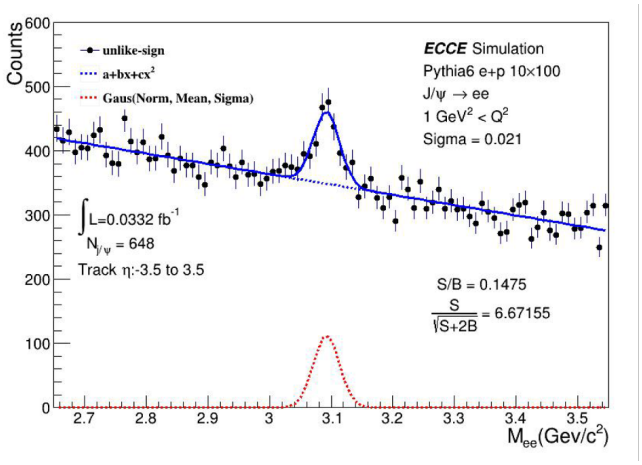

FIGURE 5. Reconstructed di-electron mass distribution in the $-3.5 \leq \eta \leq 3.5$ pseudorapidity region in 10+100 GeV $e+p$ simulation with the ECCE reference detector design performance and the 1.4 T Babar magnet. Clear J/Ψ peak can be found with the signal over background ratio at 0.148. The integrated luminosity for this distribution is 0.0332 fb^{-1}.

In addition to open heavy flavor reconstructions, feasibility studies of charmonium productions in inclusive and exclusive processes have been performed as well in $e+p$ simulation. Figure 5 shows the mass distribution of matched di-elections with the ECCE reference detector design performance in simulation for 10 GeV electron and 100 GeV proton collisions. Through the inclusive $e+p$ collisions channel and minimum Q^2 set at 1 GeV^2, around 650 J/ψs with a good signal over

background ratio can be found in $e+p$ simulation with equivalent integrated luminosity of 0.0332 fb^{-1}. The number of fully reconstructed J/ψs via the di-election decay channel in 10 fb^{-1} $e+p$ collisions at 63.2 GeV is around 0.2 million. Further studies for inclusive J/ψ reconstruction with the di-muon decay channel and their projected cross sections in different $e+p$ and $e+A$ collisions are underway.

Heavy flavor jets are usually treated as surrogates of heavy quarks produced in the partonic hard scattering processes in experiments. Comparison of heavy flavor jet yields between $e+p$ and different $e+A$ collisions will not only reveal the accessed parton distribution functions in the proton and a nucleus but also shed light on the heavy quark propagation properties in the cold nuclear medium. Both inclusive and heavy flavor jet reconstruction/tagging have been studied with the performance of the ECCE reference detector design in the 10+100 GeV $e+p$ simulation. For jet reconstruction, the anti-k_T algoritm [7] has been used and the jet cone radius ($R = \sqrt{(\eta_{jet}-\eta_{trk})^2+(\varphi_{jet}-\varphi_{trk})^2}$) is selected at 1.0 due to the low track/particle multiplicity in $e+p$ collisions at the EIC energies.

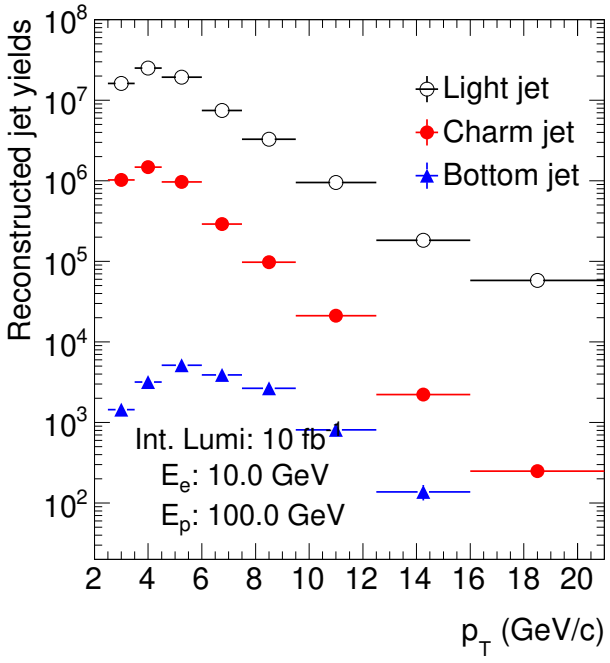

FIGURE 6. p_T distributions of reconstructed jets with different flavors in the $-3.5 \leq \eta \leq 3.5$ pseudorapidity region in 10+100 GeV $e+p$ simulation with the ECCE reference detector design performance and the 1.4 T Babar magnet. The integrated luminosity is 10 fb^{-1}. The light jet p_T spectrum is shown in black open circles, the charm jet p_T spectrum is shown in red closed circles, and the distribution of bottom jets is shown in blue closed triangles.

Charm/bottom jets are tagged if a reconstructed displaced vertex of tracks inside the jet matches with a charm/bottom hadron decay vertex, which is obtained from the PYTHIA event record, within three standard deviations of the associated vertex resolution. If there is no displaced vertex found inside the jet or the displaced vertex matching is not found, this jet is tagged as a light flavor jet. Figure 6 shows the reconstructed light jet (black open circles), charm jet (red closed circles) and bottom jet (blue closed triangles) p_T distributions in 63.2 GeV $e+p$ simulation with the ECCE reference detector design performance. These reconstructed jet yields are not corrected by the reconstruction purity and efficiency, which is under study. More than five thousand reconstructed bottom jets and more than three million charm jets can be tagged in 63.2 GeV e+p collisions with 10 fb^{-1} integrated luminosity.

3 Heavy flavor physics projection for the EIC

According to the QCD factorization mechanism [8], inclusive heavy flavor hadron cross section measurements contain the information about the accessed parton distribution functions and the sum of inclusive parton to heavy flavor hadron fragmentation functions. To directly extract the fragmentation function for a heavy quark to a particular heavy hadron formation process, the yields of reconstructed charm/bottom hadrons inside charm/bottom jets as defined in Eq. (1) have been studied in $e+p$ simulation.

$$\sigma^{e+p/A}_{h\ in\ c-jet} = \sum_a f_a^{p/A}(x,Q^2) \otimes H_{a\gamma*\to c} \otimes D^{e+p/A}_{c\to h}(z,\mu), \tag{1}$$

where $f_a^{p/A}(x,Q^2)$ is the parton distribution function for a parton with flavor a and carrying the longitudinal momentum fraction x and energy scale Q^2 inside a proton or a nucleus, $H_{a\gamma*\to c}$ is the partonic hard scattering process which can be calculated by perturbative QCD, $D^{e+p/A}_{c\to h}(z,\mu)$ is the fragmentation function for a produced parton with flavor c that forms into a hadron h with the energy/momentum fraction z relative to this parton at the fragmentation scale μ in $e+p$ or $e+A$ collisions.

The cold nuclear medium effects on the initial parton distribution functions and final state fragmentation processes can be extracted through the nuclear modification factor R_{eA} measurements of the reconstructed heavy flavor hadron inside jets, which is defined in Eq. (2).

$$R_{eA}(h\ in\ jet) = \frac{1}{A}\frac{\sigma^{e+A}_{h\ in\ jet}}{\sigma^{e+p}_{h\ in\ jet}}, \tag{2}$$

where A is the nuclear mass number and $\sigma^{e+p/A}_{h\ in\ jet}$ is the measured heavy flavor hadron in jet cross section in $e+p/A$ collisions as defined in Eq. (1).

The heavy flavor hadron in jet yields are extracted by requiring the reconstructed heavy flavor hadrons are within the cone of the reconstructed heavy flavor jets. As the $e+A$ heavy flavor event generator is still under development, the yields of reconstructed heavy flavor hadrons in jets in $e+A$ collisions are determined by the yields in $e+p$ collisions at

the same energy configuration and scaled by the associated mass number A.

Figure 7 shows the projected accuracy of the hadron momentum fraction (z_h) dependent nuclear modification factor R_{eAu} of inclusively reconstructed $D^{\pm}$ mesons in charm jets and $B^{\pm}$ mesons in bottom jets in 63.2 GeV $e+p$ and $e+Au$ collisions, in which the hadron momentum fraction, z_h, is defined as the ratio of reconstructed D meson (B meson) momentum, p_h, over the momentum of the associated charm jet (bottom jet), p_{jet}. The projected statistical uncertainties of the R_{eAu} use 10 fb^{-1} integrated luminosity for $e+p$ collisions and 500 pb^{-1} integrated luminosity for $e+Au$ collisions. The systematic uncertainties associated with different ECCE detector designs and different jet cone radius selections ($0.7 \leq R \leq 1.0$) are evaluated and shown as colored bands in Figure 7. Both charm and bottom measurements have a good coverage of the high hadron momentum fraction region ($z_h > 0.4$), which has limited constraints from existing heavy ion experimental data. With these projected integrated luminosities, reconstructed charm hadron in jet measurements can access the $z_h > 0.1$ region with better than 5% uncertainties.

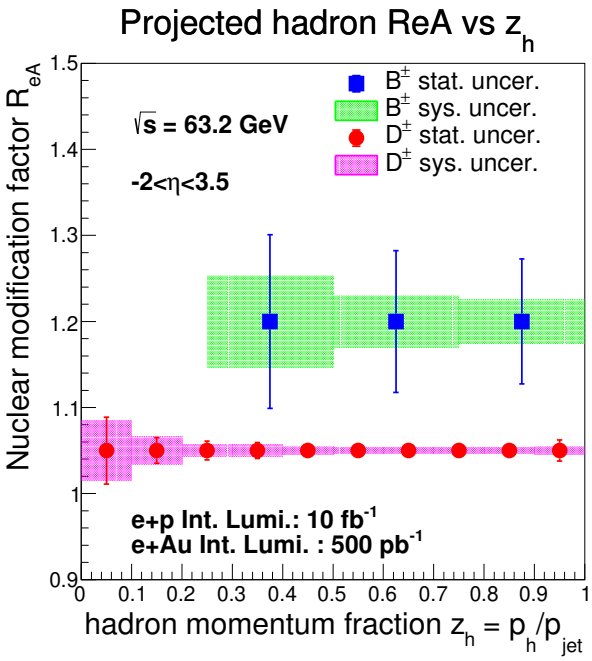

FIGURE 7. Projected statistical and systematical accuracy of inclusively reconstructed heavy flavor hadrons inside jets within the $-2 < \eta < 3.5$ pseudorapidity region in 10+100 GeV $e+p$ and $e+Au$ collisions with the ECCE reference detector design performance and the 1.4 T Babar magnet. The integrated luminosity for $e+p$ ($e+Au$) collisions is 10 fb^{-1} (500 pb^{-1}). The projected statistical uncertainties for reconstructed $D^{\pm}$ inside charm jets are shown in red closed circles and the projected statistical uncertainties for reconstructed $B^{\pm}$ inside bottom jets are shown in blue closed rectangles. The systematic uncertainties are shown in the magenta and green bands respectively.

The pseudorapidity separated hadron momentum fraction dependent R_{eAu} projections of reconstructed D^0 ($\bar{D}^0$) mesons in charm jets with the ECCE reference detector design in $e+p$ and $e+Au$ collisions at 63.2 GeV are shown in Figure 8. The statistical uncertainties are evaluated with the default ECCE reference detector design and the systematic uncertainties are calculated with different ECCE detector conceptual designs and different jet cone radii ($0.7 \leq R \leq 1.0$). The experimental projections in the $-2 < \eta < 0$ (top left), $0 < \eta < 2$ (top right) and $2 < \eta < 3.5$ (bottom left) pseudorapidity regions are compared with theoretical predictions [9] based on the parton energy loss model respectively. Better precision can be achieved by the proposed D^0 ($\bar{D}^0$) meson in charm jet measurements at the EIC than the theoretical calculations constrained by existing experimental results especially in the high hadron momentum fraction and forward pseudorapidity region. Besides the heavy flavor hadron in jet measurements, other physics observable such as the jet substructure are also under study [10] to systematically explore the kinematics dependent hadronization process.

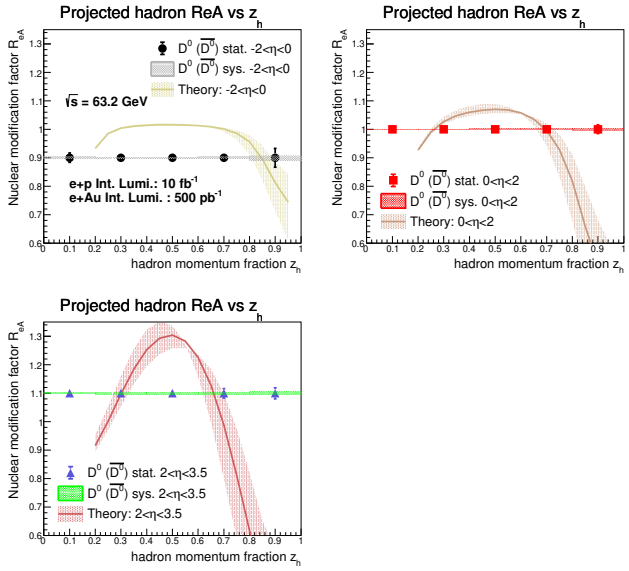

FIGURE 8. Projected statistical and systematical accuracy of the hadron momentum fraction z_h dependent reconstructed $D^0(\bar{D}^0)$ meson inside charm jets within the $-2 < \eta < 0$ (top left), $0 < \eta < 2$ (top right) and $2 < \eta < 3.5$ (bottom left) pseudorapidity regions in 10+100 GeV $e+p$ and $e+Au$ collision. The reconstructed yield are evaluated with the ECCE reference detector design and the 1.4 T Babar magnet. The integrated luminosity for $e+p$ ($e+Au$) collisions is 10 fb^{-1} (500 pb^{-1}). The theoretical calculations are from [9].

4 Summary and Outlook

A series of heavy flavor hadron and jet simulation studies have been carried out with the ECCE reference detector design. Great precision can be obtained by the proposed heavy flavor measurements at the EIC with the ECCE detector de-

sign in exploring the initial state parton distribution functions and the final state hadronization process. Better knowledge about the heavy quark fragmentation functions in different nuclear medium conditions can be provided by the heavy flavor hadron in jet measurements at the EIC especially in the not well known high hadron momentum fraction region. Following the EIC reference detector selection, joint efforts has been setup towards the EIC detector 1 technical design developments. These proposed heavy flavor simulation studies will be expanded with further updates from the EIC detector 1 design optimization and other developments.

5 Acknowledgement

We thank the EIC Silicon Consortium for cost estimate methodologies concerning silicon tracking systems, technical discussions, and comments. We acknowledge the important prior work of projects eRD16, eRD18, and eRD25 concerning research and development of MAPS silicon tracking technologies. We thank the EIC LGAD Consortium for technical discussions and acknowledge the prior work of project eRD112. We acknowledge support from the Office of Nuclear Physics in the Office of Science in the Department of Energy, the National Science Foundation, and the Los Alamos National Laboratory Laboratory Directed Research and Development (LDRD) 20200022DR.

1. A. Accardi et al., Electron Ion Collider: The Next QCD Frontier: Understanding the glue that binds us all, Eur. Phys. J. A 52 (2016) 268, 10.1140/epja/i2016-16268-9
2. R. Abdul Khalek et al., Science Requirements and Detector Concepts for the Electron-Ion Collider: EIC Yellow Report (2021)
3. S. Agostinelli et al., Geant4—a simulation toolkit, Nuclear Instruments and Methods in Physics Research Section A: Accelerators, Spectrometers, Detectors and Associated Equipment 506 (2003) 250, https://doi.org/10.1016/S0168-9002(03)01368-8
4. Fun4All, URL https://wiki.bnl.gov/sPHENIX/index.php/EIC_SPHENIX_FUN4ALL.
5. C. Pinkenburg, Analyzing Ever Growing Datasets in PHENIX, Journal of Physics: Conference Series 331 (2011) 072027, 10.1088/1742-6596/331/7/072027
6. T. Sjostrand, S. Mrenna, and P. Z. Skands, A Brief Introduction to PYTHIA 8.1, Comput. Phys. Commun. 178 (2008) 852, 10.1016/j.cpc.2008.01.036
7. M. Cacciari, G. P. Salam, and G. Soyez, The anti-k_t jet clustering algorithm, JHEP 04 (2008) 063, 10.1088/1126-6708/2008/04/063
8. J. C. Collins, D. E. Soper, and G. F. Sterman, Factorization of Hard Processes in QCD, Adv. Ser. Direct. High Energy Phys. 5 (1989) 1, 10.1142/9789814503266_0001
9. H. T. Li, Z. L. Liu, and I. Vitev, Heavy meson tomography of cold nuclear matter at the electron-ion collider, Phys. Lett. B 816 (2021) 136261, 10.1016/j.physletb.2021.136261
10. X. Li, Heavy flavor and jet studies for the future Electron-Ion Collider, PoS HardProbes2020 (2021) 175, 10.22323/1.387.0175